ORIGINAL PAPER

Graphic analysis of energy and exergy combined systems of solar collector and high-temperature heat pump

Habib Shoeibi[1] · Mehdi Mehrpooya[1,2] · Ehsanolah Assaerh[1] · Mohsen Izadi[1,3] · Fathollah Pourfayaz[1,2]

Abstract

This study investigated the heat pump system connected to the solar collector. The purpose of this study is to determine the amount of energy consumption and exergy and system performance. This system uses high-temperature heat pumps. In this paper, energy-based and exergy currents from the primary energy source to the consumer are plotted by using Sankey and Grassmann diagrams. In this article, Sankey (enthalpy flow) and Grassmann (exergy flow) diagrams of a heat pump connected to a solar collector were investigated. The results show that stream number 12 has the highest amount of exergy of the streams and the exergy destruction of the solar collector is more than other equipment and the highest energy rate is related to stream 11. Exergy analysis in thermal energy systems is very important due to the location and degree of inefficiency of the system equipment. Exergy analysis shows that the highest amount of exergy of currents with 367,092 kW is related to the inlet current of the tank and the highest amount of exergy damage of 15,563 kW equipments is related to the solar collector. This exergy destruction for solar collectors with temperature changes throughout the year with the lowest destruction in July at 14,342 kW and the highest exergy destruction at 15,678 kW is related to June. Among the rotating equipments, the most exergy damage is related to the compressor (k101) water heat transfer cycle. By changing the exergy efficiency, the amount of exergy destruction is significantly reduced.

Abbreviations

VLV-101	Expansion valve
Storage tank	Reservoir
HX2	Heat exchanger
K-101	Compressor
P-100	Pump
HX1	Heat exchanger
K-100	Compressor

List of symbols

$\dot{E}x$	Rate of exergy (kW)
$\dot{m}$	Flow rate in mass (kj/Kg)
e_i^0	Standard chemical exergy
f_b	Exergoenvironmental factor (%)

r_b	Relative environmental impacts difference (%)
e	Exergy specifics (kJ/kgmol)
E	The rate of emission
Gi	Energy from Gibbs (kj/kgmol)
h	Enthalpy specific (kj/kg)
Q	Heat task (kW)
T	Temp (K)
W	Ability (kW)
s	Entropy (kj/K)
ε	Exergy efficiency (%)
τ	Annual operating hours (h)

Subscripts

D	Exergy destruction
P	The product
F	Fuel
0	Dead state
in	Entrance
out	Output
po	Potential
ph	Physical
ch	Chemical
ke	Kinetic

✉ Mehdi Mehrpooya
mehrpoya@ut.ac.ir

1 Department of Mechanical Engineering, Dezful Branch, Islamic Azad University, Dezful, Iran

2 Renewable Energies and Environment Department, Faculty of New Sciences and Technologies, University of Tehran, Tehran, Iran

3 Mechanical Engineering Department, Faculty of Engineering, Lorestan University, Khorramabad, Iran

tot	Total
F	Fuel
P	Product
ex	Exergy

Introduction

In any industrial plant, energy flow analysis and exergy analysis and identifying equipment inefficiencies are key tools to quantify and monitor the optimal use of energy resources. To carry out such an analysis shows the amount of energy consumption is through the famous Sankey in the diagrams, where the arrows correspond to the specified values of the amount of energy consumption in the specified ranges. However, Sankey diagrams alone are not sensitive to the quality of resources and equipment, as they only reflect consumption. This issue can lead to misleading conclusions in determining inefficient equipment. One way to overcome this deficiency is to use Grassmann diagrams together with Sankey diagrams, where flows are displayed as exergy instead of energy consumption (Stegou-Sagia & Paignigiannis, 2003). Exergy analysis is also a useful tool to demonstrate the more efficient use of energy resources. A method for analyzing energy and exergy is to use Sankey and Grassmann diagrams to help policymakers and decision-makers better understand exergy and energy flow from the initial energy source to the final use (Gong & Werner 2017).

Sankey and Grassmann diagrams are an important aid in showing equipment inefficiencies and potential savings in relation to the use of energy resources. The principles of drawing Sankey diagrams follow the requirements of conservation of mass or energy. Drawing these diagrams provides a physical view of production systems and a better understanding of them. Sankey and Grassmann's analysis can show the places where exergy is lost in the cycles of industrial devices and provide valuable insights for designers of industrial devices to improve the cycle and avoid energy losses (Carrero et al. 2017; He et al. 2020; Zhang et al. 2022).

In the solar heat pump system, for effective use of solar energy, the systems are analyzed exergy. By determining the amount of reversible energy, exergy analysis can be used to improve the efficiency of a heat pump system (Imran et al. 2016; Wu et al. 2019). This method can be described as a powerful tool in the simulation of thermodynamic analysis of energy systems. In other words, it has been widely used in performance evaluation, design, and simulation of energy systems. It can be said that the maximum work that can be produced ideally for a certain amount of energy in environmental conditions in optimal conditions is exergy. Therefore, this method of analysis is a useful method for the operation design of many industrial processes (Arshad 2017) & (Alves-Filho 2015) & (Islam et al. 2019; YILMAZ, 2018).

Many researchers have investigated various exergy analysis methods in order to determine equipment inefficiency and exergy destruction rate. They have used exergy analysis methods in many renewable energy systems and different energy applications. The importance of these analysis windows has opened a separate one to focus on exergy analysis and modeling studies. In recent years, theoretical analysis based on exergy concepts and experimental studies has been done for heat pump systems.

Soundararajan et al. (Soundararajan et al., 2014) reviewed the Sankey diagram framework for energy and exergy flows. Designing and applying Sankey diagrams for any system help a lot to better understand energy loss representations at all system levels, equipment, and system energy analysis. Superimposing energy flow and exergy in Sankey diagrams provides balance estimation, calculation, and display of energy losses and identifies potential areas of energy losses and helps designers to improve their performance in these areas.

Carreroa et al. analyzed the Sankey and Grassmann diagrams in the micro-Humid Air Turbine cycle. In this research, the researchers investigated the amount of fuel consumption by drawing Sankey and Grassmann diagrams in the micro-Humid Air Turbine cycle and displayed graphically. The researcher used the graphs to visually evaluate the efficiency of the system. Vahab Ghalandari observed that the electrical work and enthalpy of the input currents have a major contribution to the total input energy of the VRM. Vahab Ghalandari graphically represented the flow of energy and exergy between sinks and sources with Sankey and Grassmann diagrams, respectively, and used the diagrams to visually evaluate system efficiency (Dincer & Rosen 2020; Ji et al. 2008; Omer 2008) &(Treichel & Cruickshank 2021) & (Cengel et al. 2019).

Koroneos Christopher and Rovas Dimitrios produced hydrogen by performing the liquefaction process. The researchers stated that the liquefaction process is very energy intensive and therefore requires a lot of exergy. By analyzing the results, the researchers showed that the hydrogen production process with the highest exergy efficiency is electrolysis using electricity from hydropower. And by analyzing the liquefaction process, they concluded that the process with the lowest exergy efficiency is driven by electrolysis by electricity from solar energy photovoltaics. By drawing a Grassmann diagram, the researchers determined the process of exergy losses in the power plant (Christopher & Dimitrios 2012).

Schmidt (Schmidt 2008) by stating that Sankey and Grassmann's diagrams are, respectively, tools for showing energy and exergy flows from the source of primary energy production to the final consumption of energy. By

drawing these graphs and analyzing them, he investigated the importance of the graphs. Marina Montero Carrero et al. (Carrero et al. 2017) thermodynamically evaluated a turbine based on Sankey and Grassmann charts. According to the results at moments of low demand, the heat allows increasing the electrical efficiency of all units of the micro-Humid Air Turbine and therefore heat production and separates the electricity. Hepbasli and Akdemir (Hepbasli & Akdemir 2004) analyzed the energy and exergy of geothermal heat pumps. The researchers drew and studied the exergy diagram (Grassmann diagram) for GSHP ground source heat pumps by analyzing the irreversibility of geothermal heat pumps. Related to heat transfer processes, in-ground heat exchanger and evaporator were compared. And this visual analysis provided the designer with a better and quantitative understanding of equipment inefficiencies and their relative values. MARIE ANHEDEN and GUNNAR SVEDBERG (Anheden & Svedberg 1998) analyzed the exergy of chemical ring combustion systems. Grassmann's diagrams were drawn for systems with gaseous coal. The researchers determined the loss and destruction of the system by examining the Grassmann diagrams.

Dmytro Harasym and Volodymyr Labay (Harasym & Labay 2015) estimated exergy efficiency and exergy losses in operational clean room air-conditioning systems by the Grassmann diagram. The Grassmann diagram allows more accurate estimation of exergy efficiency of existing air conditioning systems and exergy losses in its elements. And exergy flow and losses for existing air conditioning systems were investigated, and this investigation provides an opportunity to estimate relative exergy losses in energy technology systems and understand the type of losses. Yan et al. performed an energy and exergy analysis of a non-emission coal-fired power generation system based on coal co-gasification. They traced the exergy and energy flows of the coal system under benchmark conditions by drawing Sankey and Grassmann diagrams (Yan et al. 2015). Bonnet et al. (Bonnet et al. 2005) analyzed the energy, exergy, and cost of a micro-production system based on the Ericsson engine. They investigated the rate of exergy transfer and exergy destruction by drawing Sankey and Grassmann diagrams. By studying exergy and drawing a Grassmann diagram, Bonnet et al. investigated exergy flows and exergy destruction in the system.

Due to the importance of using fluids for heat transfer in industries and reducing exergy destruction, they conducted a variety of research in identifying and using fluids with appropriate properties and simulated in software such as Aspen HYSYS (Aghel et al. 2020; Allahyarzadeh-Bidgoli et al. 2021). Heidaryan, Ehsan et al. provided a new and reliable model for predicting fluid viscosity at high pressures and temperatures (Heidaryan, de Alcântara Pessôa Filho, & Fuentes, 2022; Heidaryan et al. 2010a, b; Heidaryan et al.

2010a, b). Research was also conducted to determine the properties of fluids with high thermal transfer efficiency to reduce exergy destruction and increase productivity coefficient (Jarrahian & Heidaryan 2012, 2014). It is well known that the convection of common fluids such as oil, water, kerosene, ethylene glycol, and a few other number of heat transfer needs are insufficient (Y. Li et al. 2020a, b; Z. Li et al. 2020a, b; Safaei et al. 2021; Zhang et al. 2022). Some researchers also examined the use of nanofluids in industry to improve the performance of war transmission (Aldabesh et al. 2021; Cao et al. 2021; Khan et al. 2021) (Iskander Tlili et al.). One way of reducing excess in industries is the use of nanofluids of different dimensions (Ali et al. 2020; Awan et al. 2021; Y. Li et al. 2020a, b). Heat transfer decreases by increasing the volume fraction of nanoparticles. Other researches show that nanofluids with CNT improve the performance of solar systems in terms of energy and exergy (Ghalandari et al. 2020; Sarafraz et al. 2019).

Stegou-Sagian,y and N. Paignigiannis (Stegou-Sagia & Paignigiannis, 2003) conducted a study on the comparison of performance in compressor and condenser by examining exergy losses in refrigeration systems. They were analyzed in the process of irreversible one-step refrigeration with refrigerant mixtures R-404A, R-410A, R-410B, and R-507 as working fluids for the vapor compression cycle. Exergy losses were calculated by a developed algorithm based on thermodynamics. The analysis of exergy balance on the components of the system is based on the parameters affecting losses, and the related results were presented in Grassmann diagrams (diagram of exergy flow rate).

Considering that, high-temperature heat pump systems with solar energy are very important in the exergy and energy analysis industries. This led us to analyze the energy and exergy of a heat pump system using Sankey and Grassmann diagrams. Graphical analysis of high-temperature heat pumps with Sankey and Grassmann diagrams can identify locations and equipment with high heat losses and help designers to increase efficiency. In the published research, the analysis is done by Sankey and Grassmann diagrams for a specific day of the year. In this research, we analyzed a solar energy heat pump in all months of the year by Sankey and Grassmann diagrams. This pump is used to produce hot water in Ahvaz pipe factory. Energy and exergy analysis was done by the graphic analysis of Sankey and Grassmann diagrams.

Materials and methods

Aspen HYSYS software was used for simulation and data analysis. This engineering software is a very powerful and accurate tool in modeling refinery, petrochemical, and electrolytic processes. The precise and powerful design method

of this software is based on packages related to different materials and their equations of state, and this powerful software displays the simulation of models and processes in a very real way. And by using the Aspen HYSYS comprehensive library, the most accurate and best simulation and analysis methods perform complex and long engineering calculations in the shortest possible time. Aspen HYSYS software data analysis is done by MATLAB software, and these two software programs are linked together. Data analysis and precise mathematical and statistical calculations with MATLAB software are of great importance. One of the features of this software is extracting input data from another software library to perform calculations based on it. Therefore, by extracting data of thermodynamic processes from Aspen HYSYS software and performing analysis in MATLAB software, more accurate exergy calculations can be achieved.

The current research has investigated the quality of energy consumption for the production of hot water in Ahvaz Pipeline Company, located in the center of Ahvaz city with about 300 sunny days. In this regard, the exergy analysis of the current situation of the above company and the procedures used to improve its energy consumption quality indicators are evaluated and analyzed by graphically drawing Sankey and Grassmann charts.

Description of the process

A heat pump with the help of indirect solar radiation is used in this study. Solar energy is an alternative to fossil fuels such as natural gas, coal, oil, and electricity. This integrated system is used for water heating applications with renewable energy. In this system, the solar collector and the heat pump together make up the water heating system of a solar heat pump. This system is made of three cycles. The first cycle includes a compound parabolic solar collector and a heat exchanger (this equipment is shared between the first cycle and the second cycle; it is an evaporator for the second cycle) and a fluid pump. The working fluid in the first cycle is oil. The working fluid transfers the heat obtained from radiant energy in the heat exchanger to the heat pump. The second cycle includes equipment, compressor, condenser (heat exchanger), expansion valve, evaporator (heat exchanger). The working fluid in this cycle is refrigerant R-134a. The third cycle includes a hot water storage tank, a water pump, and a heat exchanger (this equipment is common between the second cycle and the third cycle, and for the second cycle, it is a condenser). The working year in this cycle is water. The solar energy harvesting collector works at low temperature, but the heat pump works at high temperature, increasing its performance compared to the air source heat pump (ASHP) (Chaturvedi et al. 1982). Figure 1 shows the integrated heat pump system with compound parabolic collector (CPC) in the pipeline company. Here the collector collects solar energy and the heat collected from the sun is transferred to the secondary fluid. The refrigerant in the heat pump cycle passes through the evaporator and evaporates. The evaporated refrigerant enters the compressor and increases the pressure and temperature. Then

Fig. 1 Process of the hot water production system

the refrigerant enters the condenser and loses its heat. A decrease in temperature causes the refrigerant to evaporate and liquefy. Then the refrigerant is directed to the expansion valve so that its temperature decreases after the expansion process. The heat of the condenser is transferred to another fluid, and it transfers its heat to it and the fluid is heated.

Figure 2 shows a schematic depiction of the cycle using R-134a as the refrigerant with low boiling points. An evaporator, compressor, condenser, and expansion valve are the four main components of a typical vapor compression refrigeration cycle. The collector is exposed to direct sunlight. Upon impact with the pipelines that carry refrigerant, the sunlight is absorbed by the liquid refrigerant. In heat pumps, the constant pressure of the subcooled liquid is transformed into saturated vapor via the evaporation of the hot working fluid in the heat pump evaporator; therefore, steps (1–4) involve the transfer of heat from the working fluid to the heat pump working fluid. Process (2–3) compresses the refrigerant using the evaporator and condenser pressures. In the next step, the refrigerant is removed from the heat and condensed into a saturated liquid state under the constant pressure of (3–4). Latent heat from condensation is transferred to the circulating water from the condenser during this process. When the refrigerant passes through the relief valve, it expands, creating a mixture of liquid and vapor (Cengel et al. 2011). In industries such as refrigeration, manufacturing, and industrial applications, heat pumps have been used for decades (Treichel & Cruickshank 2021). In addition to heating homes and businesses, they are also used in heating and cooling water, refrigeration, and many industrial processes. The heat pumps compete with direct electric heating and fossil boilers in the production of heat (Chua et al. 2010; Fani et al. 2020).

With regard to the installation location of this equipment, all the aforementioned data are provided as input. A specific period of the day is chosen to take into account the collector temperature, and points are selected to calculate enthalpy values. Utilizing compressors, collectors, and thermal modules, the average monthly instantaneous values of the compressor, absorbed solar energy, and additional energy is calculated. In order to obtain annual values, the values of these parameters are integrated over a specific month and finally over all months.

Figure 2 shows the status of Ahwaz Pipeline Company's solar hot water production system and heat pump for high temperatures. There are three components to this system: The first part includes a solar compound parabolic concentrator (CPC), the second part includes a heat pump, and the third part is a storage tank. The solar radiation energy is transmitted to the CPC, and the working fluid heats the collector. To transfer the heat from the heat pump to the CPC working fluid, this fluid is pumped into the heat exchanger (evaporator). Condenser, compressor, evaporator, and expansion valve are the four main components of a vapor compression heat pump. According to this diagram, the water enters the storage and leaves after heating. Peng-Robinson equation of state has been used for process analysis in Aspen HYSYS software. Furthermore, Table 1 shows the operation condition.
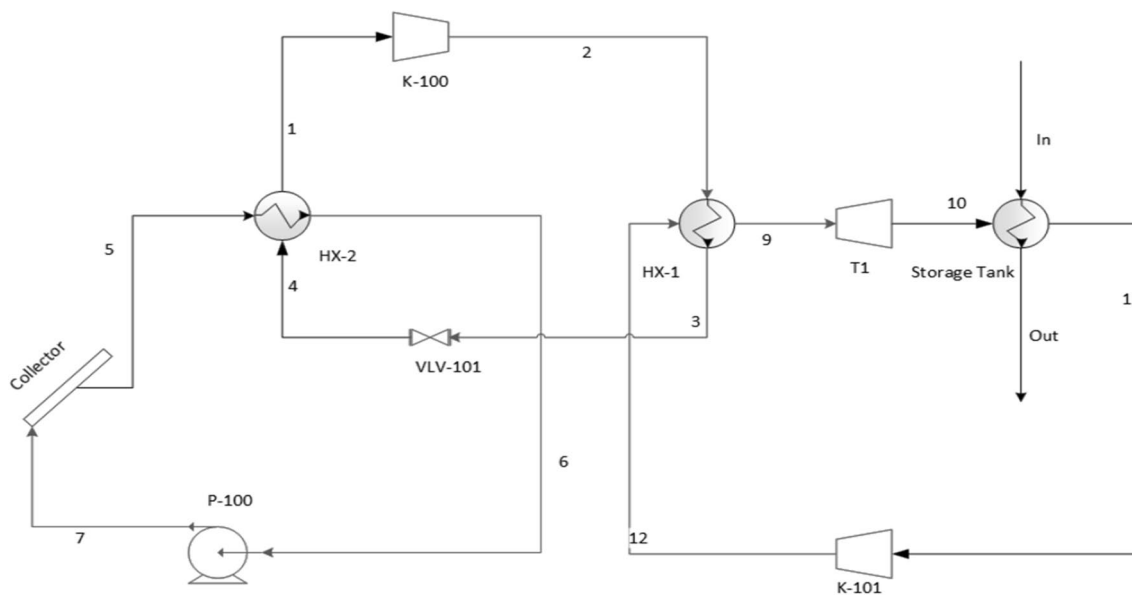

Fig. 2 Solar hot water production system of Ahvaz pipeline company

Table 1 Process data on solar hot water production system currents

Stream number	Temperature (°C)	Pressure (kPa)	Molar flow (kgmole/h)
1	274.4	150	596.6
2	329.3	400	596.6
3	88.57	400	596.6
4	88.64	150	596.6
5	275	90	596.6
6	90	90	596.6
7	90	90	596.6
8	90.01	150	596.6
9	329.3	50	1993
10	315.8	30	1993
11	40	30	1993
12	53.96	50	1993
13	53.96	50	1993
in	25	100	4432
out	99.59	100	4432

Figure 2 shows the state of the processes of the integrated solar collector system and the high-temperature heat pump of Ahvaz pipe factory. This system has three parts: The first part includes the centralized parabolic collector, the second part is the heat pump, and the third part is the storage tank. Solar radiant energy radiates to the compound parabolic concentrator (cpc) and heats the collector working fluid. This fluid transfers the heat produced in the first cycle. The heat transfer is done by entering the hot fluid into the heat exchanger (evaporator). It transfers the heat of the fluid coming out of the compound parabolic solar collector to the refrigerant of the pump. The high-temperature heat pump cycle is made up of a number of main equipment: This equipment includes a condenser (heat exchanger for the third cycle), evaporator (heat exchanger for the first cycle), expansion valve, and compressor. According to this diagram, the city water enters the tank and leaves after heating. In the analysis of processes in Hayes software, Robinson ping state equations have been used for analysis in Span Hayes software. Table 1 shows the process information of the currents of the heat pump system connected to the composite parabolic collector.

Analysis of thermodynamic

The analysis in this paper focuses on combining the two thermodynamic laws described in the concept of exergy analysis. To analyze the results in the specified conditions in the thermodynamic relationships, the following hypotheses are considered.

a. The reference (dead) mode for the system has an ambient temperature of $T_0 = 20$ C and a pressure of $P_0 = 101.325$ kPa (Weather of Ahvaz International Airport 2021).
b. The system works in steady state.
c. Changes in kinetic and gravitational conditions in energy balance and exergy are negligible.
d. Compressors and pumps are adiabatic.
e. The refrigerant (water) at the condenser outlet and the evaporator at the heat pump is saturated.
f. Pressure drop in all heat exchangers and pipelines is ignored.
g. Steady-state, constant current operation,
h. Adiabatic compressor and capillary tube,

Exergy analysis

Combining the first law with the second law of thermodynamics makes up the basis for the exergy analysis method. Energy processes in systems or equipment must be examined to determine the degree to which quality and quantity are combined. The main indicator of thermodynamic balance is exergy efficiency, which is calculated as the exergy balance of equipment or systems (Dincer & Rosen 2020; Ji et al. 2008; Omer 2008) A cyclic process is analyzed thermodynamically, and the first law of thermodynamics emphasizes the equality of work and heat as it relates to processes and systems. The premise of the first rule is that the process is possible in cycles, while natural processes that cannot be implemented in cycles can be considered (Fig. 3). Therefore, it can be said that the application of the first law of thermodynamics for a process alone does not indicate the correctness of the implementation of that process, and the first law is deficient in expressing the limitations of the implementation of thermodynamic processes or does not create any restrictions at all (Cengel et al. 2019).

Recent decades have seen extensive research devoted to energy analysis to identify equipment inefficiencies and optimize energy consumption. This analysis in the early 1970s with the onset of the energy crisis in the world with superiority over energy analysis and other methods in achieving the efficiency of energy systems due to the ability to detect irreversibility in the system and considering the quality of energy significantly. The use of energy analysis during energy conversion is to determine thermodynamic behavior (Bejan 2013). Also, in systems, it is possible to calculate the amount of irreversibility in different cycle equipment. In a system, the lower the reversibility, the better the efficiency of the system. Factors that cause irreversibility: 1-heat transfer; 2-free expansion; 3-friction due to limited degree difference; and 4-mixing of two different materials; there are other factors that cause irreversible of processes. The effects of waste and waste on electrical networks are both irreversible
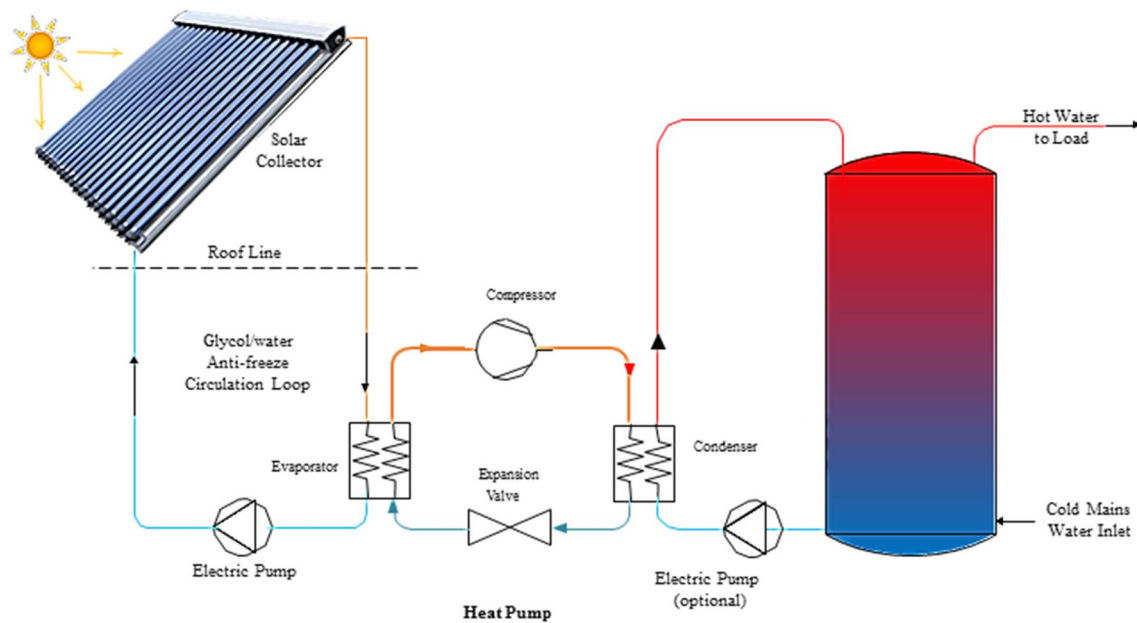
Fig. 3 Parabolic concentrated solar collector system integrated with heat pump

effects of processes. The combustion process is also an irreversible process. We must also look at the interrelationship between reversibility, balance and time. In a reversible process, the deviation from equilibrium is very small and therefore the process occurs very slowly. Because it is better for real processes to occur at limited speeds, the deviation from equilibrium must be limited. So the real process will be somewhat irreversible. The larger the deviation from the equilibrium, the greater the irreversibility and the faster the process (Sonntag et al. 2020). The lower the irreversibility in a thermodynamic process, the more work is done (or the less work required) (Dincer et al. 2004).

This analysis identifies the most inefficient equipment and shows the amount of wasted opportunities for energy use of this equipment in relation to environmental conditions, which requires clear environmental conditions (Khoshgoftar Manesh et al. 2009). Determining the characteristics of the reference environment is very important in performing system evaluation. Based on the information collected from official sources, the average reference temperature of Ahvaz city (construction site of Ahvaz Pipe Factory) is considered to be 25° C and the reference pressure is 101.325/325 K (official). Therefore, it can be concluded that exergy analysis is a fundamental method to better identify the location, causes, and extent of thermodynamic inefficiency of a process (Ghorbani et al. 2016; Safarvand et al. 2015). This analysis is a suitable method to evaluate the performance of chemical processes (Ghorbani et al. 2016).

According to Eq. (1), the exergy of each current is generally divided into four kinetic ($\dot{E}x_{ke}$), potential ($\dot{E}x_{po}$),

chemical ($\dot{E}x_{ch}$), and physical ($\dot{E}x_{ph}$) parts (Ansarinasab et al. 2017). Potential and kinetic exergy can be ignored when the system is at rest relative to its environment (Ansarinasab et al. 2017). Therefore, the exergy value of each currency can be calculated by Eq. (2) (Esen et al. 2007):

$$\dot{E}x = \dot{E}x_{po} + \dot{E}x_{ke} + \dot{E}x_{ph} + \dot{E}x_{ch} \tag{1}$$

$$\dot{E}x = \dot{E}x_{ph} + \dot{E}x_{ch} \tag{2}$$

$$\dot{E}x_{ph} = \dot{m}\left[\left(h - h_0\right) - T_0\left(s - s_0\right)\right] \tag{3}$$

In the above equations, the zero indexes represent the environmental conditions. In Eq. (3), $\dot{m}$ is mass discharge. The specific enthalpy of the reaction is h_0, the specific entropy is s_0, and the reference ambient temperature is s_0. Also in the equations below Gi is Gibbs free energy and e_i^0 is the standard chemical exergy for calculating chemical exergy (Bahram Ghorbani, Hamedi, & Amidpour, 2016; Safarvand et al. 2015). The exergy calculation of currents is shown in detail in Fig. 2.

The concept, however, enables greater exploitation of energy sources and the determination of the exact amount and location of energy lost. The concept also explains the reason for the low efficiency of the system (Anvari et al. 2017a, b).

In the case of two systems in different states, there is an opportunity for work that will continue as long as these systems are not in equilibrium. Exergy represents the

amount of work a system can produce until equilibrium is reached (Anvari et al. 2017).

The environment and the dead state are used for in order to understand exergy analysis; these two calculations are important. Pressure, chemical composition, and temperature are usually used to determine a dead state. Chemical and physical exergy of a current is calculated using the following equations (Ansarinasab et al. 2017; Nami et al. 2017).

$$e^{ph} = (h - h_0) - T_0(s - s_0) \tag{4}$$

$$E^{\dot{P}H} = \dot{m}e^{PH} \tag{5}$$

$$\dot{E}x_{ch} = \dot{m}ex_{ch} = \dot{m}\left(\sum x_i e_i^0 + G - \sum x_i G_i\right) \tag{6}$$

$$e^{ch} = \sum x_i e_i^{ch,o} + RT^O \sum x_i \ln x_i \tag{7}$$

$$E^{\dot{C}H} = \dot{m}e^{CH} \tag{8}$$

The standard chemical exergy of the current components is equal to $e_i^{ch,o}$. h, s, and o are specific enthalpies and entropies, respectively (Dincer & Cengel 2001). The chemical energy of materials is determined by obtaining the standard amount whose values are not present in the embryo. It is appropriate to think of a response that takes into account the standard chemical exergy of all reaction materials in addition to the desired material. Equation (14) is applied to the standard chemical exergy of a given material to obtain the sources (Ansarinasab et al. 2017; Kotas 2013).

These parameters will determine two important parameters of the process: energy destruction and energy efficiency that should be defined in the analysis according to Eqs. (7) and (8), and the exergy return of the equipment should be defined (Bahram Ghorbani, Hamedi, & Amidpour, 2016). These are the basic parameters for equipment (Dincer et al. 2004; Dincer & Rosen 2021).

$$\dot{E}x_D = \dot{E}x_F - \dot{E}x_P \tag{9}$$

$$\varepsilon = \frac{\dot{E}x_P}{\dot{E}x_F} = 1 - \frac{\dot{E}x_D}{\dot{E}x_F} \tag{10}$$

In the above equations, the product is shown with index P, the destruction is shown with index D, and the fuel is shown with index F.

The formulas used for the hot water production system equipment are as follows:

For compressor (Mehrpooya & Shafaei 2016; Vatani et al. 2014):

$$\dot{E}x_D = \dot{E}x_F - \dot{E}x_P = -\sum (\dot{m}.e)_{out} + \sum (\dot{m}.e)_{in} + W \tag{11}$$

$$\varepsilon = \frac{-\sum (\dot{m}.e)_{out} + \sum (\dot{m}.e)_{in}}{W} \tag{12}$$

For condenser, evaporator and heat exchangers (B Ghorbani et al. 2012):

$$\dot{E}x_D = \dot{E}x_F - \dot{E}x_P = \left[\sum (\dot{m}.e)\right]_{1,(Cold)} + \left[\sum (\dot{m}.e)\right]_{in,(Hot)} \\ - \left[\sum (\dot{m}.e)\right]_{2,(Cold)} - \left[\sum (\dot{m}.e)\right]_{out,(Hot)} \tag{13}$$

$$\varepsilon = \frac{-\left[\sum (\dot{m}.e)\right]_{out,(Hot)} + \left[\sum (\dot{m}.e)\right]_{in,(Hot)}}{-\left[\sum (\dot{m}.e)\right]_{1,(Cold)} + \left[\sum (\dot{m}.e)\right]_{2,(Cold)}} \tag{14}$$

For solar collector (Bahram Ghorbani, Hamedi, & Amidpour, 2016; Ghorbani et al. 2018):

$$\dot{E}x_D = \dot{E}x_F - \dot{E}x_P = -\sum (\dot{m}.e)_{out} + Q\left(-\frac{T}{T_0} + 1\right) + \sum (\dot{m}.e)_{in} \tag{15}$$

$$\varepsilon = \frac{Q\left(-\frac{T}{T_0} + 1\right)}{-\sum (\dot{m}.e)_{out} + \sum (\dot{m}.e)_{in}} \tag{16}$$

For expansion valve (Mehrpooya et al. 2016; Vatani et al. 2014):

$$\dot{E}x_D = \dot{E}x_F - \dot{E}x_P = \sum (\dot{m}.e)_{in} - \sum (\dot{m}.e)_{out} \tag{17}$$

$$\varepsilon = \frac{e_{out}^{\Delta T} - e_{in}^{\Delta T}}{e_{out}^{\Delta P} - e_{in}^{\Delta P}} \tag{18}$$

For pump (Mehrpooya et al. 2016; Vatani et al. 2014):

$$\dot{E}x_D = -\dot{E}x_P + \dot{E}x_F = -\sum (\dot{m}.e)_{out} + \sum (\dot{m}.e)_{in} + W \tag{19}$$

$$\varepsilon = \frac{-\sum (\dot{m}.e)_{out} + \sum (\dot{m}.e)_{in}}{W} \tag{20}$$

Thermal energy is the result of the temperature difference between the stream and its surroundings when it comes to the efficiency of the expansion valve. And the pressure component is determined by the pressure differential between the stream and the environment at the temperature of the environment.

In this regard, the properties of the main currents of the hot water production system are inlet water and heat pump outlet water.

Exergy analysis considers all components, and fuel and product are calculated according to exergy and economic objectives based on an exergy-specific costing method (Ahmadi et al. 2011).

After calculating the exergy of the fuel and the exergy of the product, the exergy variables can be calculated (Ayres et al. 1998; Calise et al. 2006; Cohce et al. 2011; Sezer & Bilgin 2013). According to the efficiency, destruction, and ratio, the exergy efficiency of component k can be determined with the exergy ratio of the fuel and the determined product (Tsatsaronis & Moran 1997):

Energy analysis

All intended equipment must comply with the specified control volume available under stable conditions. According to

Eq. (1), $\dot{m}_i$ and $\dot{m}_e$ are the mass flow inputs and outputs in the control volume, respectively (Fig. 4).

$$\sum \dot{m}_i + \sum \dot{m}_e = \frac{dm_{c.v}}{dt} \tag{21}$$

$$\sum \dot{m}_i = \sum \dot{m}_e \tag{22}$$

$$\dot{Q} + \sum (\dot{m}h)_i = \dot{W} + \sum (\dot{m}h)_e \tag{23}$$

In addition, the heat exchange and working conditions for the refrigeration cycle are considered as equations. (3) That Q and are heat exchanged and operate under the existing boundary conditions for the cycle (Goswami 2004;
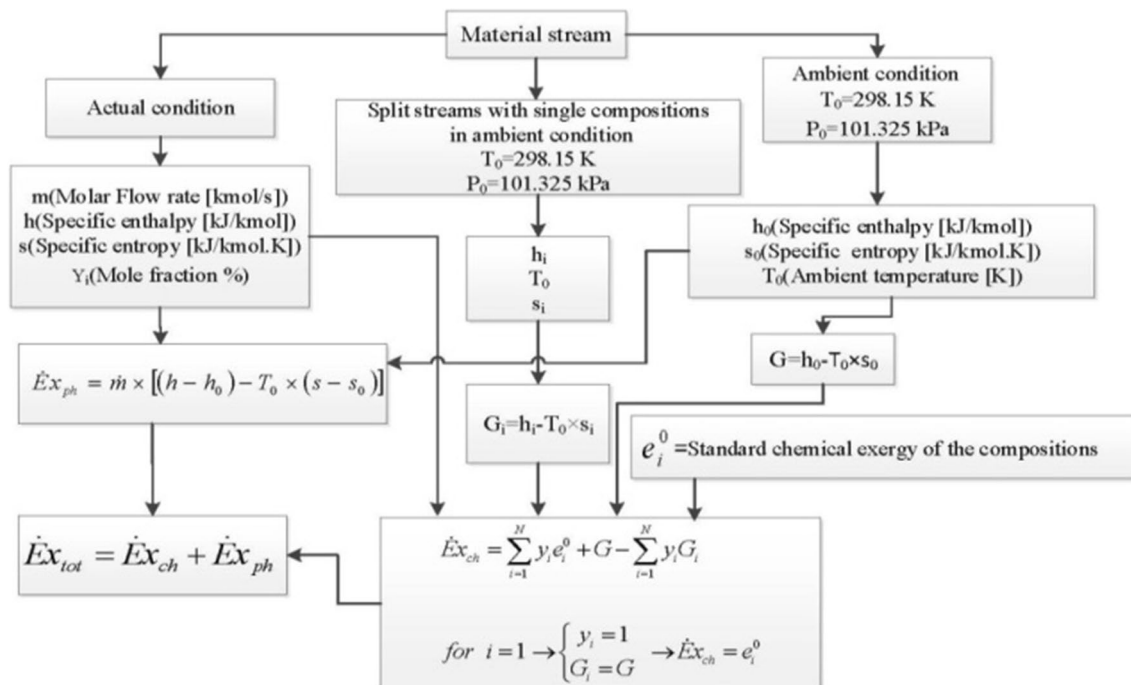
Fig. 4 Flowchart of calculating the current exergy according

Table 2 Energy equations equipments of heat pump system connected to the centralized parabolic solar collector (Cengel et al. 2011; Goswami 2004; Granet et al. 2020; MOFRAD et al. 2020; Stark 1966)

Component		Mass balance equations	Energy balances equations	Equation no
Pump	P-100	$\dot{m}_7 = \dot{m}_8 = \dot{m}_{P-100}$	$\dot{W}_{P100} = \dot{m}_{P100}(h_8 - h_7)$	(24)
Compressor	K-100	$\dot{m}_1 = \dot{m}_2 = \dot{m}_{K-100}$	$\dot{W}_{K100} = \dot{m}_{K100}(h_2 - h_1)$	(25)
	K-101	$\dot{m}_{11} = \dot{m}_{12} = \dot{m}_{K-101}$	$\dot{W}_{K101} = \dot{m}_{K101}(h_{12} - h_{11})$	(26)
Condenser, evaporator and heat exchangers	HX-2	$\dot{m}_5 = \dot{m}_6 = \dot{m}_{HX2}$	$\dot{Q}_{HX-2} = \dot{m}_{HX-2}(h_6 - h_5)$	(27)
	HX-1	$\dot{m}_2 = \dot{m}_3 = \dot{m}_{HX1}$	$\dot{Q}_{HX-1} = \dot{m}_{HX-1}(h_3 - h_2)$	(28)
	Storage tank	$\dot{m}_{11} = \dot{m}_{10} = \dot{m}_{Storage}$	$\dot{Q}_{Storage} = \dot{m}_{Storage}(h_{11} - h_{10})$	(29)
Solar collector	E-100	$\dot{m}_5 = \dot{m}_8 = \dot{m}_{Collector}$	$\dot{Q}_{Colle} = \dot{m}_{Colle}(h_5 - h_8)$	(30)
Expansion valve	valve	$\dot{m}_3 = \dot{m}_4 = \dot{m}_{VLV-101}$	$\dot{m}_3 h_3 = \dot{m}_4 h_4$	(31)

Table 3 Assumptions for calculating exergy destruction in both operational and ideal modes for compressor and heat exchanger (Kelly 2008; Tan & Keçebaş, 2014)

Components	Real conditions	Ideal conditions
Compresor	$\eta_{is} = 75\%$	$\eta_{is} = 100\%$
Heat exchanger	$\Delta T_{min} = real$	$\Delta T_{min} = 0K$
	$\Delta P = real$	$\Delta P = 0$

MOFRAD et al. 2020). Compressor consumption and turbine output work are calculated by equation (Table 2) 13 and Eq. 20, respectively, and the heat absorbed by the evaporator is determined according to Equation (Goswami 2004; MOF-RAD et al. 2020).

Discussions and results

The results of all thermodynamic analyses based on scientific principles on processes are presented in the form of defined and known indices or criteria (Table 3). One of the types of thermodynamic analysis is an energy analysis in which energy consumption is quantitatively studied and its optimality is analyzed (Cengel et al. 2019; Sonntag et al. 2020).

Figures 5, 6 and 7 show the diagrams of energy, exergy destruction, and exergy efficiency of a hot water heat pump production system connected to a solar collector.

As the next level of detail, Fig. 8 shows the components of the hot water heat pump production system connected to the solar collector. Five recurring components were discovered from the analysis of hybrid heating systems and solar heat pumps: backup heater, heat pump, and solar collector (orange fields) with a source-side (usually cold) and one-door (usually cold) storage concept, (been completed;
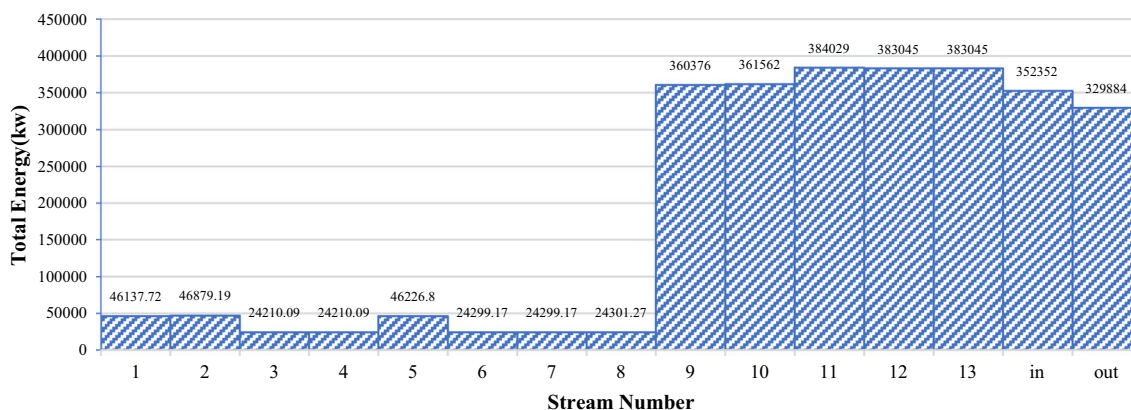
Fig. 5 Energy results of the main flows of the high-temperature heat pump system connected to the compound parabolic collector
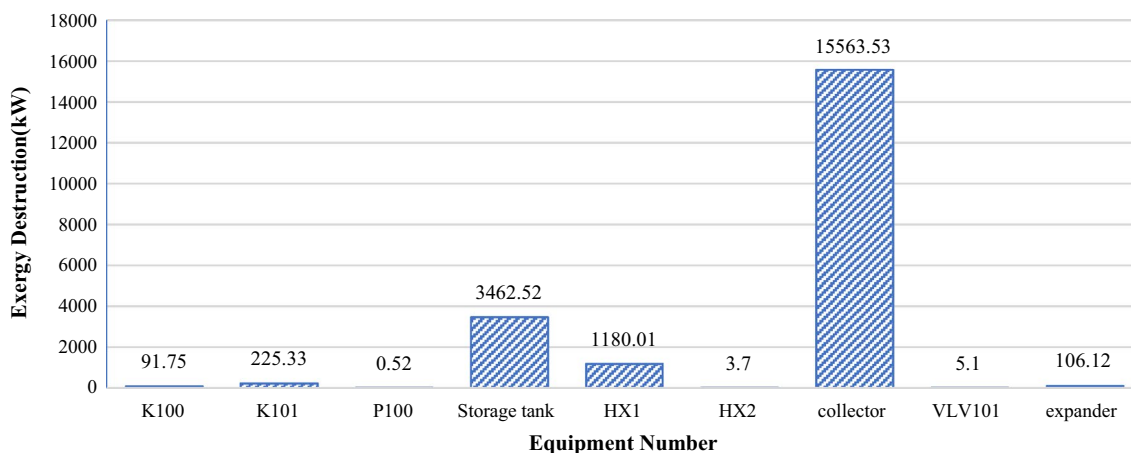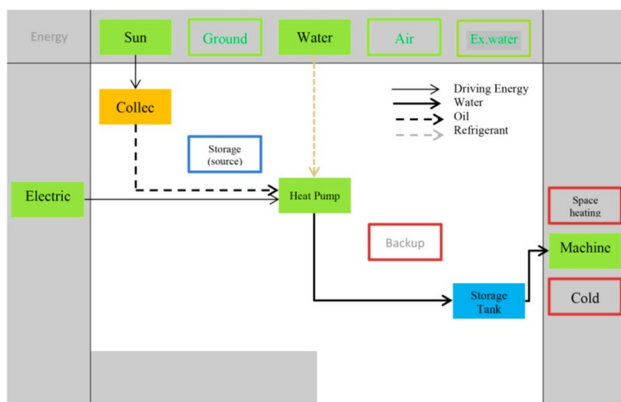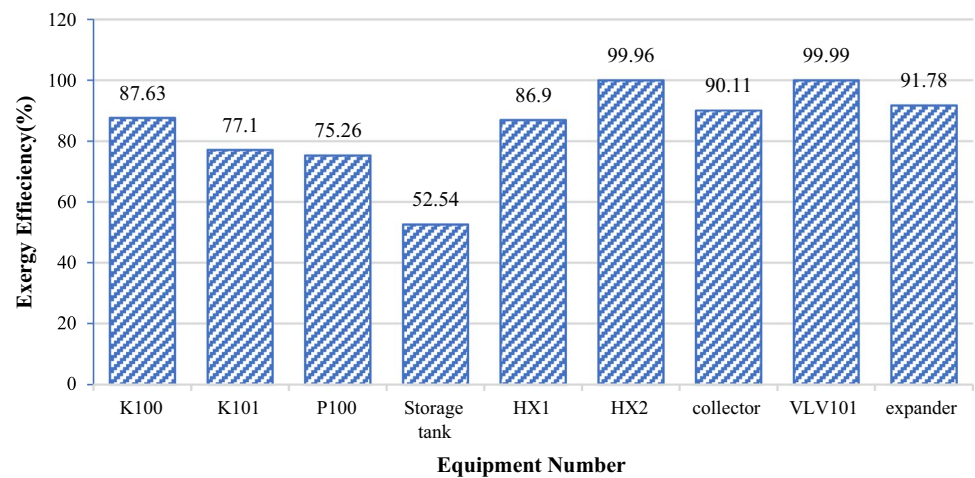
Fig. 6 Exergy destruction(kW)

Fig. 7 Exergy effieciency(%)

Fig. 8 Energy diagram of hot water heat pumps production system connected to the solar collector

usually hot) side of the heat pump sink (blue field). The positions of all these components are fixed, and if present in the concept, they can be highlighted. Any component or power source/sink that does not exist or is not used in a system is also displayed through placeholders, but is not highlighted. Different colors are used to distinguish between the final (gray): environmental energy (green) and useful (red) as well as energy converters (orange) and storage (blue). However, the information provided by coloring is not necessary to understand the concept presented.

The final step is to visualize the energy flows that connect the specific components. By doing this, this shape becomes an energy flow chart. Therefore, understanding, analysis, and last but not least, systems should be easy to compare. Each line style refers to the carrier medium, except for stimulus energies, which are mostly mass-free, for example. Solar

radiation is indifferent to the width of the lines and therefore does not represent, for example, the amount of energy transmitted. This is also true for components in general. Finally, it is important to understand that each system is represented exactly by a flowchart. This means that no specific operating modes are displayed, but all operating modes that occur in the displayed system are displayed at the same time.

Sanky and Grassmann diagrams

Image simulation of energy consumption and energy dissipation can be studied in Sanky and Grassmann diagrams. In these diagrams, based on the first and second laws of thermodynamics, the quantitative and qualitative evaluation of equipment energy is performed (Gong & Werner 2017). According to the Grassmann diagram, the amount of equipment wastage wasted and the Sankey diagram, the entropy flow in the equipment. In thermodynamic flow, the Sanky diagram contains a graphical representation of the energy distribution where the width of the arrow indicates the amount of energy distribution between the hole and the well. And it easily shows the places where the energy of the system is wasted (Osintsev & Alyukov 2022; Srinivas 2022).

A suitable method for evaluating and analyzing the second law of thermodynamics is the use of Grassmann diagrams which is similar to the Sanky diagram. The difference is that instead of entropy, the exergy current is distributed. In this graphic analysis, the places of wasted energy are easily identified and monitored (Carrero et al. 2017; Gong & Ottermo 2022). Sanky diagrams and Grassmann diagrams are tools for showing energy and exergy flows from the primary energy source to the final consumer, respectively. The Sanky diagram is an important aid in showing the ineffi- ciencies and potential savings associated with resource use
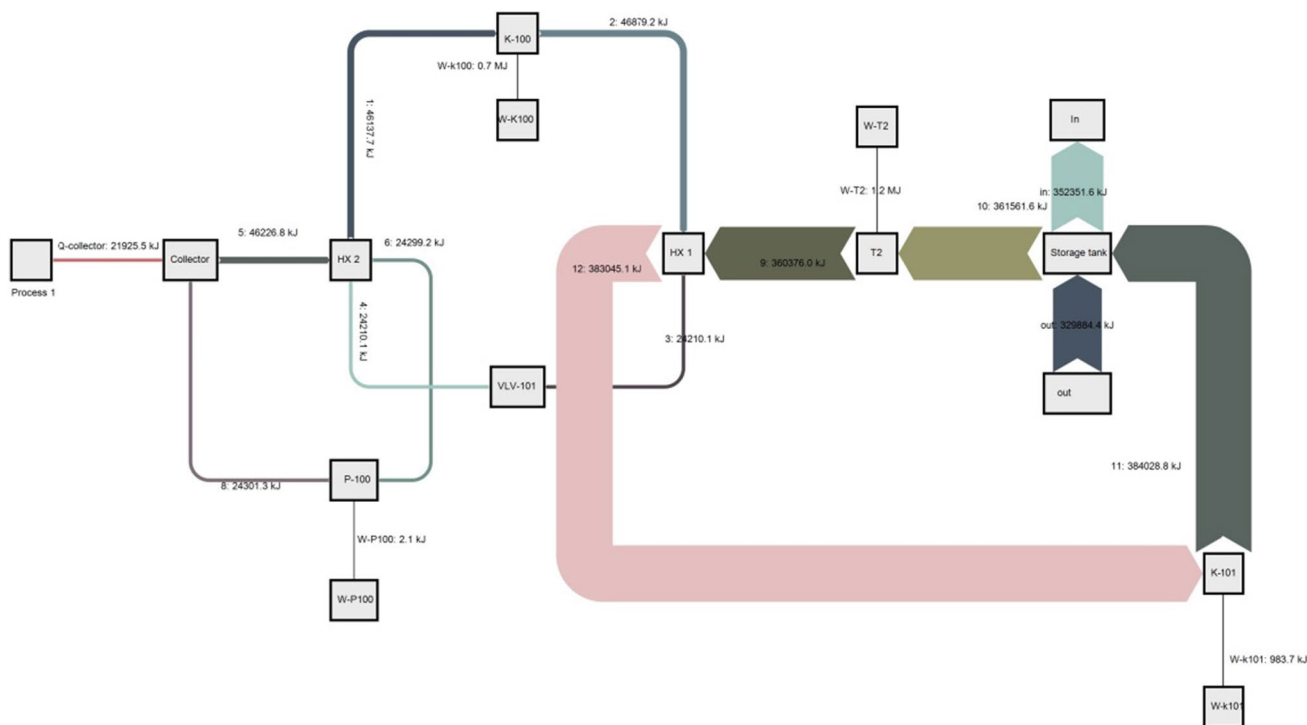
Fig. 9 The Sanky diagram shows the energy level of the system

(Osintsev & Alyukov 2022). Simple Sanky diagrams follow the requirements for energy or mass conservation and provides a physical view of production systems. The left side shows the diagram of the initial energy input currents, the middle part shows the conversion processes, and the right side shows the end users; the energy losses go from top to bottom, while the exergy destruction disappears. It becomes. nodes represented processes or distribution networks. The width of the current indicates the amount of energy/exergy. Different colors represent different types of input and output currents.

In drawing the Sankey and Grassmann diagrams, the primary energy input flows are placed on the left side of the diagram, the middle part of the transformation and transmission processes are placed, the energy consumers are placed on the right side, and the energy losses are displayed from top to bottom. There will be some. In the diagrams, the nodes, processes, or energy distribution networks between the equipment are shown. In the Sankey and Grassmann diagrams, the flow width indicates the amount of energy/exergy input and output of the equipment. Also, different colors indicate different types of input and output streams.

Figure 9 shows the Sankey diagram of the heat pump network of the high-temperature heat pump system with the help of a solar collector. In this analysis, the energy balance equation was examined for each equipment. In this diagram, the highest energy rate is related to flow 11.

Figure 10 shows the Grassmann diagram of the heat pump network with the help of the sun. In this analysis, the exergy equation was examined. Streams with thicker lines indicate the amount of exergy (stream's rat exergy flow). The narrow line shows the amount of exergy destruction of that equipment; as shown in this figure, stream number 12 has the highest amount of exergy among the streams, and the exergy destruction of the solar collector is more than other equipment. Finally, the amount of exergy destruction of the heat pump system is shown in the process block**.**

Conclusion

One of the most serious problems of human beings today is the lack of energy along with the development of modern society, which renewable and sustainable energy provides a suitable and strong solution to deal with the effects of this problem. The use of renewable energy systems in industry is very important, which minimizes energy consumption. The best option for hot water production is the use of solar energy. In this project, the use of this energy source in the field of hot water production by collectors and heat pumps has been studied.

In this study, the effect of ambient and daily reference temperature was investigated. Also, energy and exergy analysis was performed graphically and the efficiency and
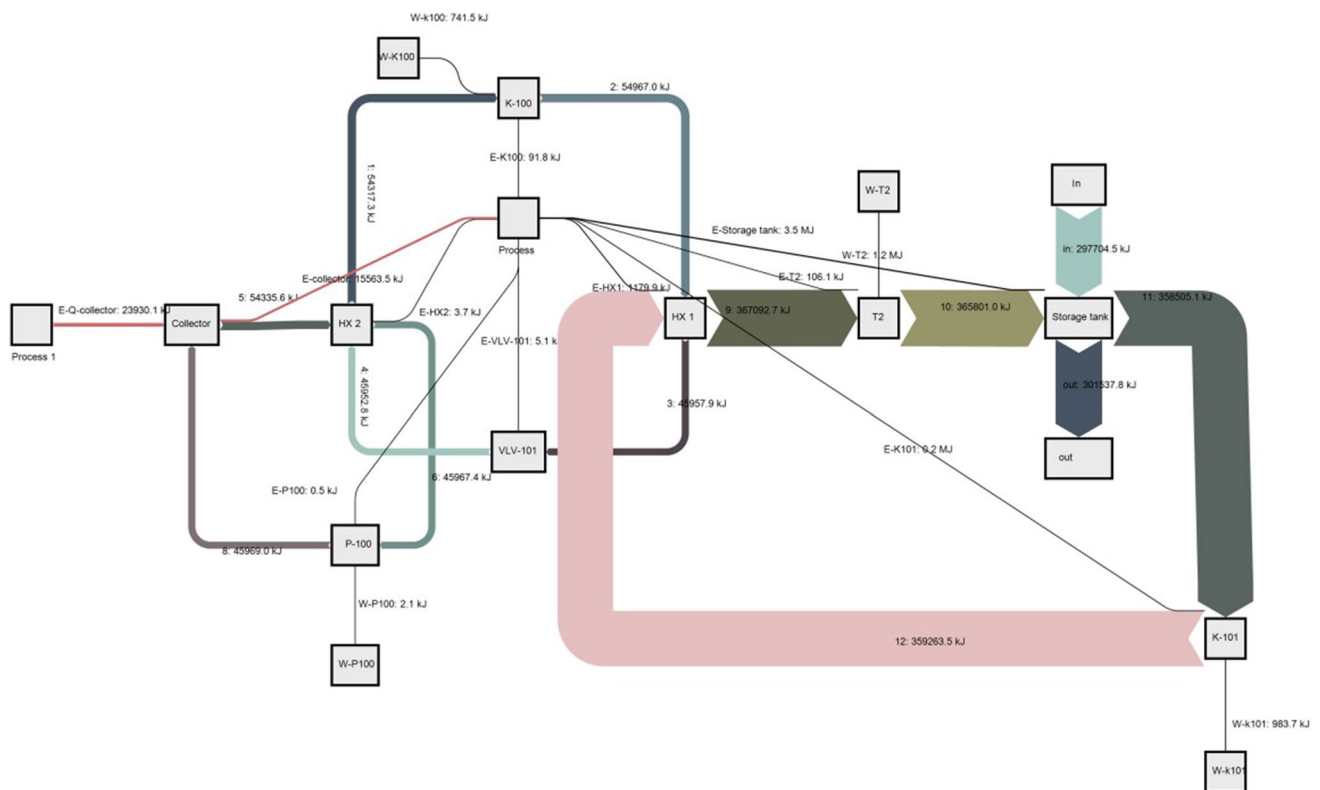
Fig. 10 The Grassmann diagram of the system exergy

ambient temperature were evaluated. This method was used to better understand the locations, causes and strategies to improve the inefficiency of the hot water production system equipment of Ahwaz Pipe Factory. The results of energy analysis and exergy in this study were observed that the most exergy damage belongs to the solar collector at 225.3 kW, while with increasing annual temperature between 25 and 55 degrees is observed that the exergy destruction of equipment varies between 0.52 and 225.3 kW Also, among the rotating equipment, the most exergy damage belongs to the K-101 compressor, which the results show that with the increase in the efficiency of this equipment, the amount of exergy damage decreases and the exergy efficiency increases. On the other hand, improving the performance of the compressor will reduce the exergy destruction more dramatically which indicates the main priority of this equipment, for better energy efficiency.

In this paper, energy-based and exergy currents from the primary energy source to the consumer are plotted using Sankey and Grassmann diagrams. The graphs show that more than half of the exergy source in the solar collector is destroyed. In the industrial heating system, the maximum

exergy efficiency of the heat pump is when entering using the sun. The pump uses a lot of renewable energy sources.

Declarations

Conflict of interest The authors declared no conflict of interest.

Ethical approval There were no ethical considerations to be considered in this research.

References

Aghel B, Sahraie S, Heidaryan E (2020) Carbon dioxide desorption from aqueous solutions of monoethanolamine and diethanolamine in a microchannel reactor. Sep Purif Technol 237:116390. https://doi.org/10.1016/j.seppur.2019.116390

Ahmadi P, Dincer I, Rosen MA (2011) Exergy, exergoeconomic and environmental analyses and evolutionary algorithm based

multi-objective optimization of combined cycle power plants. Energy 36(10):5886–5898. https://doi.org/10.1016/j.energy.2011.08.034

Aldabesh A, Hussain M, Khan N, Riahi A, Khan SU, Tlili I (2021) Thermal variable conductivity features in Buongiorno nanofluid model between parallel stretching disks: improving energy system efficiency. Case Stud Therm Eng 23:100820. https://doi.org/10.1016/j.csite.2020.100820

Ali M, Rad MM, Nuhait A, Almuzaiqer R, Alimoradi A, Tlili I (2020) New equations for Nusselt number and friction factor of the annulus side of the conically coiled tubes in tube heat exchangers. Appl Therm Eng 164:114545. https://doi.org/10.1016/j.applthermaleng.2019.114545

Allahyarzadeh-Bidgoli A, Heidaryan E, Yanagihara JI, Pessôa Filho P (2021) Assessment of correlations and simulation software to calculate phase diagrams of pre-salt fluids. Pet Sci Technol 39(11–12):410–420. https://doi.org/10.1080/10916466.2021.1906700

Alves-Filho O (2015) Heat pump dryers: theory, design and industrial applications. CRC Press, Florida

Anheden M, Svedberg G (1998) Exergy analysis of chemical-looping combustion systems. Energy Convers Manag 39(16–18):1967–1980. https://doi.org/10.1016/S0196-8904(98)00052-1

Ansarinasab H, Mehrpooya M, Mohammadi A (2017a) Advanced exergy and exergoeconomic analyses of a hydrogen liquefaction plant equipped with mixed refrigerant system. J Clean Prod 144:248–259

Ansarinasab H, Mehrpooya M, Parivazh MM (2017b) Evaluation of the cryogenic helium recovery process from natural gas based on flash separation by advanced exergy cost method–Linde modified process. Crygenious 87:1–11

Anvari S, Saray RK, Bahlouli KJATE (2017a) Employing a new optimization strategy based on advanced exergy concept for improvement of a tri-generation system. Appl Therm Eng 113(1452):1463. https://doi.org/10.1016/j.applthermaleng.2016.11.146

Anvari S, Taghavifar H, Parvishi AJ (2017b) Management thermo-economical consideration of regenerative organic Rankine cycle coupling with the absorption chiller systems incorporated in the trigeneration system. Energy Convers Manag 148:317–329. https://doi.org/10.1016/j.enconman.2017.05.077

Arshad M (2017) Clean and sustainable energy technologies. In Clean energy for sustainable development (pp. 73–89): Elsevier. https://doi.org/10.1016/B978-0-12-805423-9.00003-X

Awan AB, Zubair M, Memon ZA, Ghalleb N, Tlili I (2021) Comparative analysis of dish Stirling engine and photovoltaic technologies: energy and economic perspective. Sustain Energy Technol Assess 44:101028. https://doi.org/10.1016/j.seta.2021.101028

Ayres RU, Ayres LW, Martinás K (1998) Exergy, waste accounting, and life-cycle analysis. Energy 23(5):355–363. https://doi.org/10.1016/S0360-5442(97)00076-5

Bejan A (2013) Convection heat transfer. Wiley, Hoboken

Bonnet S, Alaphilippe M, Stouffs P (2005) Energy, exergy and cost analysis of a micro-cogeneration system based on an Ericsson engine. Int J Therm Sci 44(12):1161–1168. https://doi.org/10.1016/j.ijthermalsci.2005.09.005

Calise F, Palombo A, Vanoli L (2006) Design and partial load exergy analysis of hybrid SOFC–GT power plant. J Power Sources 158(1):225–244. https://doi.org/10.1016/j.jpowsour.2005.07.088

Cao Y, Mihardjo LW, Dahari M, Tlili I (2021) Waste heat from a biomass fueled gas turbine for power generation via an ORC or compressor inlet cooling via an absorption refrigeration cycle: a thermoeconomic comparison. Appl Therm Eng 182:116117. https://doi.org/10.1016/j.applthermaleng.2020.116117

Carrero MM, De Paepe W, Bram S, Parente A, Contino F (2017) Does humidification improve the micro Gas Turbine cycle? Thermodynamic assessment based on Sankey and Grassmann diagrams. Appl Energy 204:1163–1171. https://doi.org/10.1016/j.apenergy.2017.05.067

Cengel YA, Boles MA, Kanoğlu M (2011) Thermodynamics: an engineering approach. McGraw-hill, New York

Cengel YA, Boles MA, Kanoğlu M (2019) Thermodynamics: an engineering approach. McGraw-hill, New York

Chaturvedi SK, Chiang YF, Roberts As, Jr (1982). Analysis of two-phase flow solar collectors with application to heat pumps. J Sol Energy Eng 104(4):358–365

Christopher K, Dimitrios R (2012) A review on exergy comparison of hydrogen production methods from renewable energy sources. Energy Environ Sci 5(5):6640–6651. https://doi.org/10.1039/C2EE01098D

Chua KJ, Chou SK, Yang W (2010) Advances in heat pump systems: a review. Appl Energy 87(12):3611–3624. https://doi.org/10.1016/j.apenergy.2010.06.014

Cohce M, Dincer I, Rosen M (2011) Energy and exergy analyses of a biomass-based hydrogen production system. Biores Technol 102(18):8466–8474. https://doi.org/10.1016/j.biortech.2011.06.020

Dincer I, Cengel YA (2001) Energy, entropy and exergy concepts and their roles in thermal engineering. Entropy 3(3):116–149. https://doi.org/10.3390/e3030116

Dincer I, Rosen MA (2020) Exergy energy, environment and sustainable development. Newnes, Londan

Dincer I, Rosen MA (2021) Thermal energy storage systems and applications. Wiley, Hoboken

Dincer I, Hussain M, Al-Zaharnah IJ (2004) Energy and exergy use in public and private sector of Saudi Arabia. Energy Policy 32(14):1615–1624. https://doi.org/10.1016/S0301-4215(03)00132-0

Esen H, Inalli M, Esen M, Pihtili K (2007) Energy and exergy analysis of a ground-coupled heat pump system with two horizontal ground heat exchangers. Build Environ 42(10):3606–3615. https://doi.org/10.1016/j.buildenv.2006.10.014

Fani M, Norouzi N, Ramezani M (2020) Energy, exergy, and exergoeconomic analysis of solar thermal power plant hybrid with designed PCM storage. Int J Air-Conditioning Refrigeration 28(04):2050030. https://doi.org/10.1142/S2010132520500303

Ghalandari M, Maleki A, Haghighi A, Shadloo MS, Nazari MA, Tlili I (2020) Applications of nanofluids containing carbon nanotubes in solar energy systems: a review. J Mol Liq 313:113476. https://doi.org/10.1016/j.molliq.2020.113476

Ghorbani B, Salehi G, Ghaemmaleki H, Amidpour M, Hamedi M (2012) Simulation and optimization of refrigeration cycle in NGL recovery plants with exergy-pinch analysis. J Nat Gas Sci Eng 7:35–43. https://doi.org/10.1016/j.jngse.2012.03.003

Ghorbani B, Hamedi M-H, Amidpour M (2016a) Exergoeconomic evaluation of an integrated nitrogen rejection unit with LNG and NGL co-production processes based on the MFC and absorbtion refrigeration systems. Gas Process J 4(1):1–28

Ghorbani B, Hamedi M-H, Amidpour M (2016b) Development and optimization of an integrated process configuration for natural gas liquefaction (LNG) and natural gas liquids (NGL) recovery with a nitrogen rejection unit (NRU). J Nat Gas Sci Eng 34:590–603

Ghorbani B, Shirmohammadi R, Mehrpooya M (2018) A novel energy efficient LNG/NGL recovery process using absorption and mixed refrigerant refrigeration cycles–Economic and exergy analyses. Appl Therm Eng 132:283–295. https://doi.org/10.1016/j.applthermaleng.2017.12.099

Gong M, Ottermo F (2022) High-temperature thermal storage in combined heat and power plants. Energy. https://doi.org/10.1016/j.energy.2022.124057

Gong M, Werner S (2017) Mapping energy and exergy flows of district heating in Sweden. Energy Procedia 116:119–127. https://doi.org/10.1016/j.egypro.2017.05.060

Goswami DY (2004) The CRC handbook of mechanical engineering. CRC Press, Florida

Granet I, Alvarado JL, Bluestein M (2020) Thermodynamics and heat power. CRC Press, Florida

Harasym D, Labay V (2015) the estimation of exergy efficiency and exergy losses in air conditioning systems of operating cleanrooms by a grassmann diagram. Energy Eng Control Syst 1(1):1–8

He W, Namar MM, Li Z, Maleki A, Tlili I, Shadloo MS (2020) Thermodynamic analysis of a solar-driven high-temperature steam electrolyzer for clean hydrogen production. Appl Therm Eng 172:115152. https://doi.org/10.1016/j.applthermaleng.2020.115152

Heidaryan E, Moghadasi J, Salarabadi A (2010a) A new and reliable model for predicting methane viscosity at high pressures and high temperatures. J Nat Gas Chem 19(5):552–556. https://doi.org/10.1016/S1003-9953(09)60109-2

Heidaryan E, Salarabadi A, Moghadasi J, Dourbash A (2010b) A new high performance gas hydrate inhibitor. J Nat Gas Chem 19(3):323–326. https://doi.org/10.1016/S1003-9953(09)60060-8

Heidaryan E, de Alcântara Pessôa Filho P, Fuentes MDR (2022) Molecular dynamic simulations of clathrate hydrate structures i: lattice constant and thermal expansion. J Low Temp Phys 207(5):227–240. https://doi.org/10.1007/s10909-022-02725-9

Hepbasli A, Akdemir O (2004) Energy and exergy analysis of a ground source (geothermal) heat pump system. Energy Convers Manage 45(5):737–753. https://doi.org/10.1016/S0196-8904(03)00185-7

Imran M, Usman M, Park B-S, Lee D-H (2016) Volumetric expanders for low grade heat and waste heat recovery applications. Renew Sustain Energy Rev 57:1090–1109. https://doi.org/10.1016/j.rser.2015.12.139

Islam M, Yarlagadda P, Karim A (2019) Effect of the orientation schemes of the energy collection element on the optical performance of a parabolic trough concentrating collector. Energies 12(1):128. https://doi.org/10.3390/en12010128

Jarrahian A, Heidaryan E (2012) A novel correlation approach to estimate thermal conductivity of pure carbon dioxide in the supercritical region. J Supercrit Fluids 64:39–45. https://doi.org/10.1016/j.supflu.2012.02.008

Jarrahian A, Heidaryan E (2014) A simple correlation to estimate natural gas thermal conductivity. J Nat Gas Sci Eng 18:446–450. https://doi.org/10.1016/j.jngse.2014.04.005

Ji J, Pei G, Chow T-T, Liu K, He H, Lu J, Han C (2008) Experimental study of photovoltaic solar assisted heat pump system. Sol Energy 82(1):43–52. https://doi.org/10.1016/j.solener.2007.04.006

Kelly S (2008) Energy systems improvement based on endogenous and exogenous exergy destruction. Berlin, D38.

Khan SU, Tlili I, Waqas H, Imran M (2021) Effects of nonlinear thermal radiation and activation energy on modified second-grade nanofluid with Cattaneo-Christov expressions. J Therm Anal Calorim 143(2):1175–1186. https://doi.org/10.1007/s10973-020-09392-6

Khoshgoftar Manesh M, Amidpour M, Hamedi MJ (2009) Optimization of the coupling of pressurized water nuclear reactors and multistage flash desalination plant by evolutionary algorithms and thermoeconomic method. Int J Energy Res 33(1):77–99. https://doi.org/10.1002/er.1475

Kotas TJ (2013) The exergy method of thermal plant analysis. Elsevier, Netherlands

Li Y, Waqas H, Imran M, Farooq U, Mallawi F, Tlili I (2020a) A numerical exploration of modified second-grade nanofluid with motile microorganisms, thermal radiation, and Wu's slip. Symmetry 12(3):393. https://doi.org/10.3390/sym12030393

Li Z, Sarafraz M, Mazinani A, Moria H, Tlili I, Alkanhal TA, Safaei MR (2020b) Operation analysis, response and performance evaluation of a pulsating heat pipe for low temperature heat recovery. Energy Convers Manage 222:113230. https://doi.org/10.1016/j.enconman.2020.113230

Mehrpooya M, Shafaei AJ (2016) Advanced exergy analysis of novel flash based Helium recovery from natural gas processes. Energy 114:64–83. https://doi.org/10.1016/j.energy.2016.07.169

Mehrpooya M, Lazemzade R, Sadaghiani MS, Parishani H (2016) Energy and advanced exergy analysis of an existing hydrocarbon recovery process. Energy Convers Manag 123:523–534. https://doi.org/10.1016/j.enconman.2016.06.069

Mofrad KG, Zand S, Salehİ G, Maneshİ MH (2020) Comparative 4E and advanced exergy analyses and multi-objective optimization of refrigeration cycles with a heat recovery system. Int J Thermodyn 23(3):197–214. https://doi.org/10.5541/ijot.749471

Nami H, Nemati A, Fard FJ (2017) Conventional and advanced exergy analyses of a geothermal driven dual fluid organic Rankine cycle (ORC). Appl Therm Eng 122:59–70. https://doi.org/10.1016/j.applthermaleng.2017.05.011

official, A. m. Retrieved from https://www.ahvaz.ir/

Omer AM (2008) Energy, environment and sustainable development. Renew Sustain Energy Rev 12(9):2265–2300. https://doi.org/10.1016/j.rser.2007.05.001

Osintsev K, Alyukov S (2022) Experimental investigation into the exergy loss of a ground heat pump and its optimization based on approximation of piecewise linear functions. J Eng Phys Thermophys 95(1):9–19. https://doi.org/10.1007/s10891-022-02451-9

Safaei MR, Tlili I, Gholamalizadeh E, Abbas T, Alkanhal TA, Goodarzi M, Dahari M (2021) Thermal analysis of a binary base fluid in pool boiling system of glycol–water alumina nano-suspension. J Therm Anal Calorim 143(3):2453–2462. https://doi.org/10.1007/s10973-020-09911-5

Safarvand D, Aliazdeh M, Samipour Giri M, Jafarnejad MJAP (2015) Exergy analysis of NGL recovery plant using a hybrid ACOR-BP neural network modeling: a case study. J Chem Eng 10(1):133–153. https://doi.org/10.1002/apj.1857

Sarafraz M, Safaei MR, Leon AS, Tlili I, Alkanhal TA, Tian Z, Arjomandi M (2019) Experimental investigation on thermal performance of a PV/T-PCM (photovoltaic/thermal) system cooling with a PCM and nanofluid. Energies 12(13):2572. https://doi.org/10.3390/en12132572

Schmidt M (2008) The Sankey diagram in energy and material flow management: part II: methodology and current applications. J Ind Ecol 12(2):173–185. https://doi.org/10.1111/j.1530-9290.2008.00015.x

Sezer İ, Bilgin A (2013) Effects of charge properties on exergy balance in spark ignition engines. Fuel 112:523–530. https://doi.org/10.1016/j.fuel.2012.09.078

Sonntag RE, Borgnakke C, Van Wylen GJ, Van Wyk S (2020) Fundamentals of thermodynamics. Wiley, New York

Soundararajan K, Ho HK, Su B (2014) Sankey diagram framework for energy and exergy flows. Appl Energy 136:1035–1042. https://doi.org/10.1016/j.apenergy.2014.08.070

Srinivas T (2022) Exergy analysis of a HDH-VCR cycle for water and air conditioning. Int J Exergy 37(1):40–56. https://doi.org/10.1504/IJEX.2022.120107

Stark J (1966). Fundamentals of classical thermodynamics (van wylen, gordon j.; sonntag, richard e.). In: ACS Publications

Stegou-Sagia A, Paignigiannis N (2003) Exergy losses in refrigerating systems A study for performance comparisons in compressor

and condenser. Int J Energy Res 27(12):1067–1078. https://doi.org/10.1002/er.936

Tan M, Keçebaş A (2014) Thermodynamic and economic evaluations of a geothermal district heating system using advanced exergy-based methods. Energy Convers Manage 77:504–513. https://doi.org/10.1016/j.enconman.2013.10.006

Treichel C, Cruickshank CA (2021) Energy analysis of heat pump water heaters coupled with air-based solar thermal collectors in Canada and the United States. Energy 221:119801. https://doi.org/10.1016/j.energy.2021.119801

Tsatsaronis G, Moran MJ (1997) Exergy-aided cost minimization. Energy Convers Manage 38(15–17):1535–1542. https://doi.org/10.1016/S0196-8904(96)00215-4

Vatani A, Mehrpooya M, Palizdar A (2014) Advanced exergetic analysis of five natural gas liquefaction processes. Energy Convers Manag 78:720–737. https://doi.org/10.1016/j.enconman.2013.11.050

Weather of Ahvaz International Airport. (2021). Retrieved from https://weawow.com/fa/

Wu Z, Zhang Y, Deng N (2019) Performance investigation of the heat pump and power generation integration system. Int J Energy Res 43(14):8608–8622. https://doi.org/10.1002/er.4858

Yan L, Yue G, He B (2015) Exergy analysis of a coal/biomass co-hydrogasification based chemical looping power generation system. Energy 93:1778–1787. https://doi.org/10.1016/j.energy.2015.10.042

Yilmaz H (2018) Optimization of an integral flat plate collector storage system for domestic solar water heating in Adana. Anadolu Üniversitesi Bilim Ve Teknoloji Dergisi A-Uygulamalı Bilimler Ve Mühendislik 19(1):165–176. https://doi.org/10.18038/aubtda.335801

Zhang J, Sajadi SM, Chen Y, Tlili I, Fagiry MA (2022) Effects of Al_2O_3 and TiO_2 nanoparticles in order to reduce the energy demand in the conventional buildings by integrating the solar collectors and phase change materials. Sustainable Energy Technol Assess 52:102114. https://doi.org/10.1016/j.seta.2022.102114